Preparation of C_{60} Ribbons by in situ Crystallization in a Microfluidic System

Kyosuke Shinohara,[1] Takeshi Fukui,[1] Hiroaki Abe,[2] Naoto Sekimura,[1] and Koji Okamoto[1]
[1]*Department of Quantum Engineering and Systems Science, The University of Tokyo, 7-3-1 Hongo, Bunkyo-ku, Tokyo 113-8656*
[2]*Department of Nuclear Engineering and Management, The University of Tokyo, 7-3-1 Hongo, Bunkyo-ku, Tokyo 113-8656*

(Received June 28, 2006; CL-060730; E-mail: shinohara@vis.k.u-tokyo.ac.jp)

This letter reports a fabrication method for C_{60} crystalline thin ribbons using a microfluidic system. The bulk size of the C_{60} ribbons is controlled by hydrodynamic force.

Recently, fullerene C_{60} has attracted much attention because of its unique physical and chemical properties.[1–4] Processing and control of C_{60} solid materials on a macroscopic scale is a major technical challenge. Here, we demonstrate a fabrication method for size-controlled C_{60} ribbons on a microchip.

The fabrication method for the C_{60} ribbons is based on microfluidic liquid/liquid interfacial precipitation (LLIP).[5] Figure 1 shows a schematic of the experimental setup. The test solutions used were C_{60} dissolved in toluene and in methanol. The raw C_{60} material used was a commercial 99.5% C_{60} powder (Honjo Chemical Co., Tokyo, Japan). The concentration of C_{60} dissolved in toluene was constant at 0.58 mg/mL (0.13 mol %). Both two solutions were maintained at a low temperature of 0 °C using a temperature controller until just prior to introduction into the channels. Toluene and methanol were introduced into a Y-shaped glass microchannel with dimensions of 100-μm width, 40-μm depth, and 40-mm length fabricated on quartz glass by wet etching (ICC-SY05, Institute of Microchemical Technology Co., Kawasaki, Japan).[6] The microchannel was immersed in a water bath, and a water immersion objective lens (Olympus LUMPlanFl $M = 100$x, $NA = 1.0$, Olympus Co., Tokyo, Japan) was used for in situ observations. In the LLIP method, needle-like C_{60} crystals are usually formed at the toluene/isopropyl alcohol (IPA) interface.[7] Conversely, when methanol was used as the solvent alcohol solution, polyhedron particles rather than needle-like crystals were formed.[5]

To form the liquid/liquid interface, each solution was introduced using syringe pumps at the same flow rate. In terms of fluid dynamics, the confluence point of the Y-junction shown by the arrow ("Nucleation Point" in Figure 1) was the stagnation point, where the velocity of fluid flow was zero. As a result, polyhedral crystalline particles were assembled at the Y-junction point of the microchannel, and they formed the seeds for the C_{60} crystalline ribbons. (Figure 2). The C_{60} ribbons grew along the toluene/methanol interface. For a total flow rate of 1.5 μL/min (Figure 2a), the C_{60} crystal grew in the streamwise and spanwise directions. While the streamwise crystal growth continued, the spanwise crystal growth stagnated gradually. Conversely, for the total flow rate of 60 μL/min, spanwise crystal growth was much smaller (Figure 2b). Since the fluid flow was fast compared to diffusion of the dissolved C_{60} molecules across the interface, the spanwise crystal growth was inhibited in this case. The streamwise crystal growth rate was determined by the flow rate, i.e., flow velocity of the test fluids (Figure 2c). As the fluid velocity increased, the growth rate increased and gradually became constant. This tendency was in agreement with that in previous experimental observations of crystal growth of potash alum ($AlK(SO_4)_2 12H_2O$) on a bulk scale.[8] The crystal growth of C_{60} ribbons thus consisted of both a solvent-mediated process limited by mass transport and a nonsolvent-mediated process limited by heat transfer.

Hydrodynamic forces in microfluidic chips were recently utilized for control of the morphology of materials, such as microtubes,[9] nonspherical particles,[10] multicore capsules,[11]

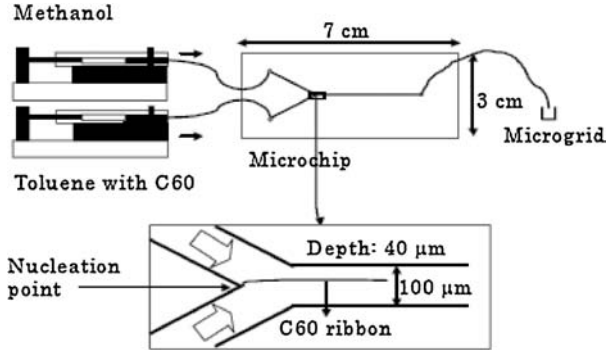

Figure 1. Schematic of experimental setup.

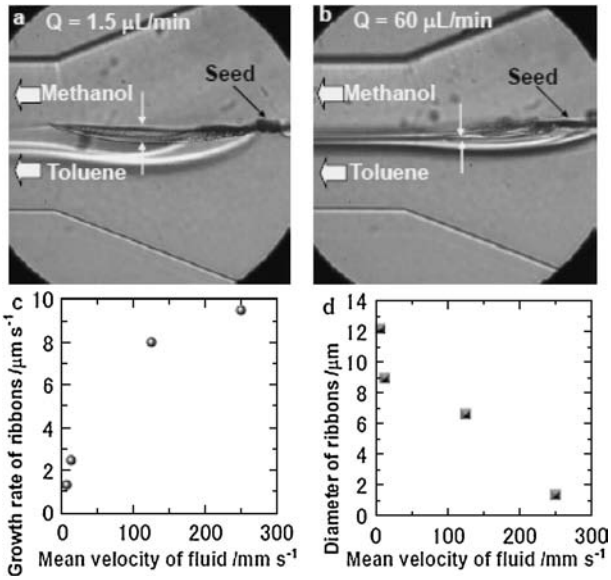

Figure 2. Optical micrographs of C_{60} ribbons and characterization by fluid velocity. Q is total flow rate. The corresponding Reynolds numbers are (a) 0.81 at $Q = 1.5$ μL/min and (b) 32.4 at $Q = 60$ μL/min, respectively.

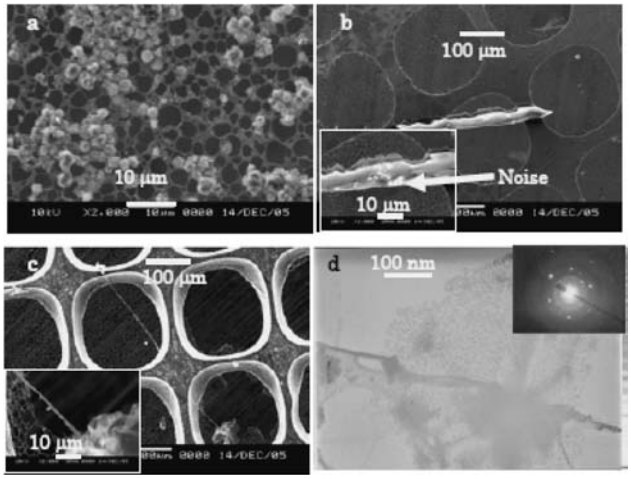

Figure 3. Scanning electron micrographs and transmission electron micrograph of the seed and C_{60} ribbons.

Janus bicolor particles,[12] Janus rods,[13] etc. In this work as well, hydrodynamic force was a key factor for the preparation of the size-controlled C_{60} crystalline ribbons. The diameter of the crystalline ribbon was determined by the fluid velocity (Figure 2d). As the mean fluid velocity increased, spanwise diffusion time across the interface decreased. In result, the spanwise crystal growth was inhibited, and the diameter of the ribbon decreased.

Scanning electron microscopy (SEM) and transmission electron microscopy (TEM) revealed the characteristics of the C_{60} ribbons and their seed. Figure 3a shows polyhedral particles, which assembled at the confluence point of the microchannel. The diameter was 3–6 μm. Shapes formed included hexagonal plates, cubic, cuboid, octahedron, etc. Under a low flow rate condition, sword-like C_{60} ribbon was produced (Figure 3b). The length and diameter was 220 and 13 μm, respectively. On the surface of the ribbon, a number of particles were observed (Figure 3b, inset). At the bottom of the ribbon, some image noise marked by arrow was observed. This was a result of evaporation of the surface film by the electron beam, indicating that the ribbon was very thin. Under a high flow rate condition, thinner C_{60} ribbon was formed (Figure 3c) with length and diameter 400 and 1.2 μm, respectively. This ribbon had a twisted morphology (Figure 3c, inset). Video imaging showed crystal growth of several ribbons from different seeds (Figure 2b is a frame). They overlapped with each other along the toluene/methanol interface. In previous work, the generation of complex three-dimensional flow fields at the liquid/liquid interface in a microchannel owing to differences in the surface tension and viscosity was reported.[14] In the present study as well, we assumed that three-dimensional flow fields at the interface were generated, and they led to the helical and multilayered morphology of the C_{60} ribbon.

Figure 3d shows a TEM image of the surface of the C_{60} ribbon shown in Figure 3b. The ribbon was covered by a thin film. The current microfluidic preparation method thus was effective in fabricating high-quality ordered C_{60} crystals as in the previous methods.[15]

In summary, we have developed a microfluidic system for the fabrication of size-controlled crystalline C_{60} ribbons. The size was controlled by the spanwise diffusion time and hydrodynamic force. In future work, we will attempt to investigate the optical and electrical properties of the ribbons and apply them to practical devices.

The authors thank the Grant-in-Aid from the Japan Society for the Promotion Science, Japan.

References

1 A. F. Hebard, M. J. Rosseinsky, R. C. Haddon, D. W. Murphy, S. H. Glarum, T. T. M. Palstra, A. P. Ramirez, A. R. Kortan, *Nature* **1991**, *350*, 600.
2 G. B. Alers, B. Golding, A. R. Kortan, R. C. Haddon, F. A. Theil, *Science* **1992**, *257*, 511.
3 L. Akselrod, H. J. Byrne, C. Thomson, *Chem. Phys. Lett.* **1993**, *212*, 384.
4 V. Capozzi, G. Casamassima, G. F. Lourusso, *Solid State Commun.* **1996**, *98*, 853.
5 K. Shinohara, T. Fukui, H. Abe, N. Sekimura, K. Okamoto, *Langmuir* **2006**, *22*, 6477.
6 a) H. Hisamoto, T. Saito, M. Tokeshi, A. Hibara, T. Kitamori, *Chem. Commun.* **2001**, 2662. b) M. Ueno, H. Hisamoto, T. Kitamori, S. Kobayashi, *Chem. Commun.* **2003**, 936. c) J. Kobayashi, Y. Mori, K. Okamoto, R. Akiyama, M. Ueno, T. Kitamori, S. Kobayashi, *Science* **2004**, *304*, 1305.
7 a) K. Miyazawa, Y. Kuwasaki, A. Obayashi, M. Kuwabara, *J. Mater. Res.* **2002**, *17*, 83. b) S. H. Lee, K. Miyazawa, R. Maeda, *Carbon* **2005**, *43*, 887.
8 a) J. W. Mullin, J. Garside, *Trans. Inst. Chem. Eng.* **1967**, *45*, T285. b) J. Garside, R. Janssen-Van Rossmalen, P. Bennema, *J. Cryst. Growth* **1975**, *29*, 353.
9 W. Jeong, J. Kim, S. Kim, S. Lee, G. Mensing, D. J. Beebe, *Lab on a Chip* **2004**, *4*, 576.
10 S. Xu, Z. Nie, M. Seo, P. Lewis, E. Kumacheva, H. A. Stone, P. Garstecki, D. B. Weibel, I. Gitlin, G. M. Whitesides, *Angew. Chem., Int. Ed.* **2005**, *44*, 724.
11 Z. Nie, S. Xu, M. Seo, P. Lewis, E. Kumacheva, *J. Am. Chem. Soc.* **2005**, *127*, 8058.
12 T. Nisisako, T. Torii, T. Takahashi, Y. Takizawa, *Adv. Mater.* **2006**, *18*, 1152.
13 D. Dendukuri, D. C. Pregibon, J. Collins, T. Alan Hatton, P. S. Doyle, *Nat. Mater.* **2006**, *5*, 365.
14 K. Shinohara, Y. Sugii, A. Aota, A. Hibara, M. Tokeshi, T. Kitamori, K. Okamoto, *Meas. Sci. Technol.* **2004**, *15*, 1965.
15 a) C. Reber, L. Yee, J. McKiernan, J. I. Zink, R. S. Williams, W. M. Tong, D. A. A. Ohlberg, R. L. Whetten, F. Diederich, *J. Phys. Chem.* **1991**, *95*, 2127. b) W. M. Tong, D. A. A. Ohlberg, H. K. You, R. S. Williams, S. J. Anz, M. M. Alvarez, R. L. Whetten, Y. Rubin, F. N. Diederich, *J. Phys. Chem.* **1991**, *95*, 4709. c) Y. Achiba, T. Nakagawa, Y. Matsui, S. Suzuki, H. Shiromaru, K. Yamauchi, K. Nishiyama, M. Kainosho, H. Horii, *Chem. Lett.* **1991**, 1233. d) E. J. Snyder, M. S. Anderson, W. M. Tong, R. S. Williams, S. J. Anz, M. M. Alvarez, Y. Rubin, R. N. Diederich, R. L. Whetten, *Science* **1991**, *253*, 171. e) A. Skumanich, *Chem. Phys. Lett.* **1991**, *182*, 486. f) T. Ichihashi, K. Tanigaki, T. Ebbesen, S. Kuroshima, S. Iijima, *Chem. Phys. Lett.* **1992**, *190*, 179.

Published on the web (Advance View) September 2, 2006; doi:10.1246/cl.2006.1108